Time-resolved emission spectroscopy in laser-generated nitrogen plasmas

R. C. Alam, S. J. Fletcher, K. R. Wasserman, and L. Hüwel
Department of Physics, Wesleyan University, Middletown, Connecticut 06457-6036
(Received 6 November 1989)

Extremely high-lying states of atomic and molecular nitrogen ions have been observed and analyzed in the transient plasma that results from focusing a Q-switched Nd:YAG (where YAG denotes yttrium aluminum garnet) laser into a pure nitrogen atmosphere ranging in pressure from 100 to 800 Torr. During the first 10 to 80 ns after plasma ignition several states of N^{3+} can be detected. Their Stark broadened linewidth is strongly time dependent due to the rapidly changing electron density in the decaying plasma. At around 20 to 40 μs after plasma ignition, rotationally resolved emission in the first negative system of N_2^+, $B\,^2\Sigma_u^+ \rightarrow X\,^2\Sigma_g^+$ indicates a rotational and vibrational temperature of about 9500 K. No significant interference from the second positive system $C\,^3\Pi_u \rightarrow B\,^3\Pi_g$ of the neutral molecule is observed. Under these conditions rotational levels up to $N'=112$ in the R branch of the (0,0) band have been identified. In this band, new perturbations at around $N'=82$ and 95 due to the $v=12$ and 13 vibrational levels of the $A\,^2\Pi_u$ state are reported.

I. INTRODUCTION

It only took a few years after the Q-switched laser was invented[1,2] to realize experimentally that the enormous electric-field strengths going along with it are capable—in particular upon additional focusing—to readily ionize and dissociate atoms and molecules. The physics of laser-triggered gas breakdown was so soon the focus of intense research that already in 1969 a review article on the subject quoted 161 relevant papers.[3] Investigations of this effect have led to such diverse applications as fusion research,[4] or new methods in analytical chemistry,[5] and x-ray laser schemes.[6] In all of these endeavors a large fraction of the available knowledge stems from the application of more or less standard spectroscopic techniques and information to these laser plasmas. Since a large amount of energy is being deposited in a very small volume and in a very short time, the highly perturbed system is usually very complex and exhibits dramatic spatial and temporal gradients in almost all characteristic parameters. It may be because of these complexities that laser-generated plasmas have not been widely used as the source for new spectroscopic information—with the notable exception of the spectroscopy of multiply charged ions which greatly benefits from the search for x-ray lasers. This scarcity of new spectroscopic data is particularly obvious in the case of molecules since it is usually found that the plasma "temperatures" are too elevated to allow for any significant molecular emission. Nevertheless, a few spectroscopic studies of laser breakdown in molecular gases have been published that mention the occurrence of molecular emission.[7–9]

In the present paper we report new spectroscopic information on nitrogen atomic and molecular ions, obtained from time-resolved emission spectroscopy following gas breakdown in pure nitrogen. A 10-Hz Nd:YAG (where YAG denotes yttrium aluminum garnet) laser operating at $\lambda=1064$ nm, with up to 500 mJ per pulse is focused through an aspherical lens with $f=10$ cm into a small chamber containing high-purity N_2. Emission of the ensuing plasma is imaged onto the entrance slits of various dispersing instruments, recorded in real time, and suitably averaged and stored. Depending on gas pressure, laser power density, time of observation (with $t=0$ being plasma "ignition"), and position of the sampled volume within the plasma plume, very different features are detected. At "early" times ($t \leq 80$ ns) emission from the $3p\,^3P$ and $3p\,^3P^\circ$ states of N^{3+} is readily detected between 344.36 and 348.47 nm. The Stark broadening of these lines has been investigated and compared to recently reported results.[10] At nitrogen pressures of 250 Torr and delay times larger than about 40 ns, the N^+ line at 343.81 nm corresponding to the $3p\,^1S \rightarrow 3s\,^1P$ transition is blended into the $3p\,^3P-3s\,^3P^\circ$ multiplet. The character of the emission spectrum changes dramatically as the plasma expands and cools. After passing through a phase of predominantly atomic (singly charged and neutral) emission, the "late" times of the plasma ($t \geq 20$ μs) are dominated by the first negative system of the molecular nitrogen ion. Reduced in overall intensity by several orders of magnitude, the $B\,^2\Sigma_u^+ \rightarrow X\,^2\Sigma_g^+$ transition is still clearly resolvable since it is remarkably free from interference of any other atomic or molecular emission; particularly noteworthy is the almost complete absence of the second positive system that is commonly found together with the $N_2^+(B\text{-}X)$ bands. Despite the significant cooling of the ambient plasma, the nitrogen ion is found to emit at a rotational and vibrational temperature of about 9500 K. At this temperature rotational levels of up to $N=112$ have been clearly identified. New information on the perturbation by the $A\,^2\Pi_u$ state has been obtained. Combined with high-resolution spectrometers or subsequent laser probing—which unfortunately was not in the realm of the current work—the laser-plasma source has tremendous potential as a source for probing details of the coupling between electron and nuclear motion in highly rotationally excited states. Another question that we have addressed in the current paper but which will undoubted-

ly profit from further investigation is the problem of achieving and/or maintaining local thermodynamic equilibrium even for the highest rotational levels under conditions of extremely rapid change.

II. EXPERIMENTAL

The experimental setup and procedure can be understood with the help of Fig. 1. Essentially, there are four major components associated with this experiment: the laser to generate the transient plasma, the gas handling system and breakdown chamber where the plasma is actually located, the monochromator or spectrometer for wavelength dispersion, and finally the electronics to capture and store the data in real time. Some of the details that are relevant for the experiment will be described below. Briefly, the usual sequence of the experiment is as follows: A pulse from the Nd:YAG laser is focused into the small gas chamber where under suitable conditions it produces electrical breakdown of the gas. The subsequent plasma emission is imaged onto the entrance slit of a wavelength-dispersing instrument. In operation mode I the time-dependent emission intensity of a small wavelength band—which is determined by the instrument settings—is recorded with a fast digital storage oscilloscope. In mode II a gated integrator is used to recover portions of interest of the emission spectrum during a well-defined period of time. Alternatively, a gated optical multichannel analyzer was used to record wavelength-dispersed spectra. In all cases the timing trigger is provided by the Q-switched Nd:YAG laser. After suitable averaging, the data are output as hard copies and/or stored for future analysis on disk.

A Q-switched, amplified Nd:YAG laser (1) (numbers in parentheses refer in this paragraph to Fig. 1) operating at 1064 nm, with a pulse width of about 15 ns and near-Gaussian beam profile is directed through the center of an aspherical lens (2) with 10-cm focal length which is optimized for the YAG fundamental. Usage of such a lens avoids the well-documented problem of multiple focal spots.[11] After passing through an antireflection coated window, about 97% of the pulse energy leaving the laser is delivered into the focal volume. This energy is typically of the order of 300 mJ. With an estimated beam diameter of 10 mm these parameters lead to power densities in the focal region of around 10^{10} to 10^{12} W cm^{-2}. The small portion of the laser pulse that is not absorbed in the plasma plume is reflected by an absorbing glass disk into a beam dump (3).

Ultra-high-purity nitrogen gas is introduced into a small stainless-steel vessel (4) with a total volume of about 4000 cm^3. A convection-type gauge monitors the gas pressure with an accuracy of about $\pm 5\%$. The focal region and hence the location of the laser-produced plasma inside the chamber are placed at or near the center, thus allowing easy alignment and viewing through two side windows (5) that are attached perpendicular to the laser direction. The window facing the monochromator and the lenses (6) to image the plasma plume onto the entrance slit are made from high-quality quartz. The focal lengths of the two imaging lenses are chosen to optimize collection efficiency ($f_1 = 15$ cm) and coupling to the monochromator optics ($f_2 = 12$ cm). Thus, a slight reduction in the image size is present. The monochromator used in most of the experiments reported here has a focal length of 60 cm. Its entrance and exit slits are adjusted to 30 μm for maximum resolution—which has been determined experimentally by scanning over well-isolated lines in several hollow cathode lamps under low-current conditions. A consistent value of 0.035 nm was found. A 1200-lines/mm grating blazed for 560 nm is used for all runs with this monochromator. A few survey runs were done with an optical multichannel analyzer (OMA) connected to a 0.25-m spectrometer with a resolution of about 1.5 nm.

The signal at the exit slit of the monochromator is

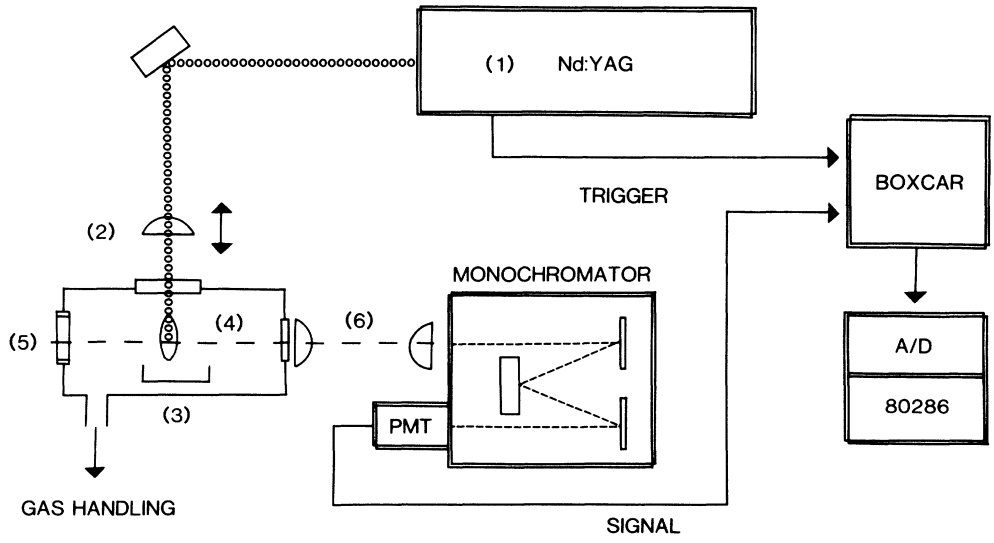

FIG. 1. Schematic representation of experimental setup for mode IIa operation: (1) pulsed Nd:YAG laser, (2) best-form lens, (3) laser beam dump, (4) gas cell, (5) alignment and viewing ports, (6) imaging lenses. See text for further details.

detected by a photomultiplier with bialkali photocathode and an intrinsic rise time of about 3 ns. The photomultiplier signal is processed in two different ways according to the data acquisition mode employed. In order to obtain the time dependence of certain emission features (mode I), the photomultiplier output is fed into a 100-MHz digital storage oscilloscope with averaging capabilities. Typically, the averaged signal of the continuous background in the vicinity of the emission feature in question is also accumulated for eventual base line subtraction. Wavelength-dispersed spectra are obtained at well-specified intervals of time in two different ways (mode IIa and IIb). In the first setup the photomultiplier viewing the scanning monochromator is connected to a boxcar integrator with adjustable delay and gate width. The averaged analog output of the boxcar integrator is then stored via analog-to-digital conversion board into a microcomputer where further analysis and data display are managed (mode IIa). For a limited number of experiments, a gated optical multichannel analyzer integrated with a 0.25-m spectrometer was available (mode IIb). Triggering of the gating electronics in this instance was accomplished with the same timing pulse from the Nd:YAG laser as in mode IIa.

In order to calibrate the wavelength reading of the monochromator, extensive scans in the wavelength range from about 395 to 335 nm were accumulated with a standard Fe hollow cathode lamp. More than 70 Fe and Ne (fill gas) lines have been identified[12] in this wavelength region. Care was taken that in these calibration runs the same scan and data acquisition parameters were used as in the actual scans with the laser plasma. With the Fe line at 381.58 nm taken as the reference position, all lines were observed with reproducibilities of better than 0.01 nm.

III. STARK BROADENING OF N^{3+}

It is well known that laser-generated plasmas—in particular in the early phases of their existence and when produced at solid surfaces—can include multiply charged ions.[13,14] Obviously, the schemes to produce short-wavelength lasers with laser plasmas take advantage of this fact. What is less frequently exploited is the possibility to investigate the Stark-broadening behavior of such species in surroundings of high electron density. Stark broadening of neutral and singly ionized atoms is a thoroughly studied phenomenon because of its basic scientific interest as well as its usefulness for plasma diagnostic.[15] Nevertheless, the Stark-broadening behavior of multiply charged ions and their role in high density plasmas is not well understood. We have observed line broadening of high-lying states in N^{3+} at electron densities estimated to be in the range from 10^{16} to 10^{18} cm^{-3}. Previously unknown Stark-broadening behavior of several lines in N III, IV, and V has been reported only recently for a few values of electron densities from studies of a linear-pinch nitrogen discharge plasma.[10] Two of these transitions, namely, the $3p\ ^3P^\circ \rightarrow 3s\ ^3S$ and the $3p\ ^3P \rightarrow 3s\ ^3P^\circ$ multiplets, have been observed in our experiments during the early stages ($t \leq 80$ ns) of laser sparks in pure nitrogen at pressures between 100 and 500 Torr. Examples of experimental and calculated spectra are shown in Fig. 2. The data in this figure were obtained by scanning the monochromator with a slew rate of 0.24 nm/min while the laser was focused into 250 Torr of N_2. Emission from the center of the visible plasma plume was detected with the boxcar gate adjusted in this particular run to a nominal width of 2 ns and a delay of 40 ns after ignition. As can be seen from the figure, the emission lines are extremely broad—widths in excess of 0.2 nm have been observed (compare Ref. 9). It was also found that they can only be fit satisfactorily with Lorentzian line shapes, indicating that Doppler broadening is not dominant despite the high electron and ion temperatures at these early stages of the plasma. Even at temperatures around 10^5 K the calculated Doppler broadening at 345 nm for ionic N is only about 0.02 nm. The least-square-fitted spectrum in Fig. 2 is a multiparameter function

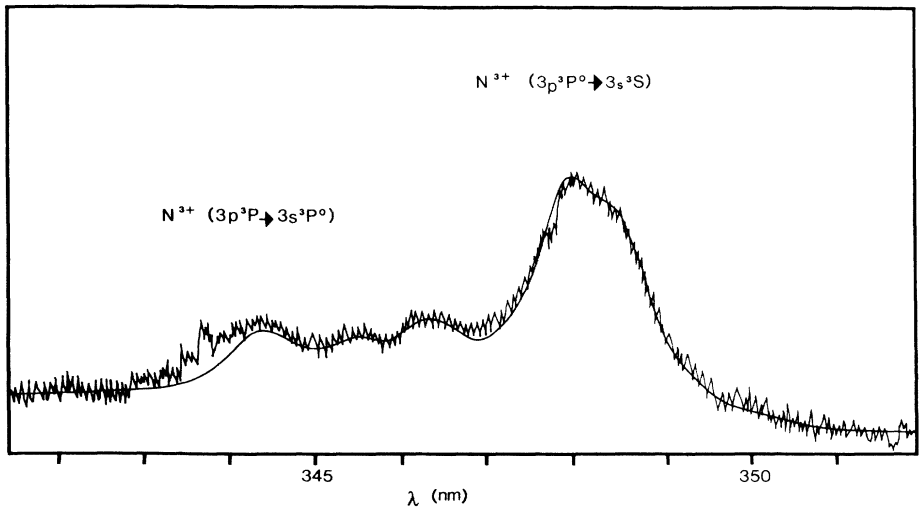

FIG. 2. N^{3+} emission at 40 ns after plasma ignition and nitrogen pressure of 250 Torr. The solid line is the least-square-fitted sum of Lorentzians centered at the line components of the $3p\ ^3P-3s\ ^3P^\circ$ and the $3p\ ^3P^\circ-3s\ ^3S$ arrays with FWHM of 0.25 and 0.28 nm, respectively.

representing two groups of Lorentzians for the two N^{3+} multiplets and the continuum background which was approximated as a sloped straight line over the short range of the fit. In the linear-pinch experiment[10] the Stark width of several nitrogen lines—including an N IV line—was shown to increase from around 0.01 nm to about 0.3 nm when the electron density was increased from about 2×10^{17} cm^{-3} to a value of 1.4×10^{18} cm^{-3}. The full width at half maximum (FWHM) values at around 40 ns in the present work are therefore consistent with electron densities of the order of 10^{18} cm^{-3}. Data taken at delay times of up to about 100 ns exhibit a gradual decrease in the observed linewidths and a dramatic intensity reduction of the N^{3+} lines due to diminishing electron density and plasma temperature. All these data can be fit with the same group of Lorentzians used in Fig. 2. Also obvious from these runs is the emergence of the $N^{+}(2p3p\ ^1S\rightarrow 2p3s\ ^1P^{\circ})$ emission line at 343.7 nm. This particular line is already present at 40-ns delay, as can be seen in Fig. 2 where it accounts for the difference between observed and calculated emission intensity at the corresponding wavelength.

What obviously is a drawback of the laser-produced plasma—its high degree of inhomogeneity and rapid change—can also be regarded as an advantage. To the extent that sampling volume and integration time are kept sufficiently small the plasma can be regarded as quasihomogeneous and stationary. Then the fact that the plasma is cooling implies the possibility of measuring quantities that depend on electron temperature and density—such as Stark widths—as a function of a parameter that varies continuously over a large range. In principle, it is possible to measure independently the local electron density in the plasma[16] so that "delay time after plasma ignition" can be calibrated in terms of the average electron density during that time.

IV. NITROGEN FIRST NEGATIVE SYSTEM

There are very few references in the laser-plasma literature to the observation of molecular emission. This is undoubtedly due to the high electron and ion temperatures that prevail in laser-produced plasmas and minimize the presence of molecular species. Some observations refer to molecular nitrogen emission stemming from photoexcitation of the cooler regions surrounding the plasma core.[17] We report here rotationally resolved emission spectra from the $B\ ^2\Sigma_u^+$ state of N_2^+ which appears a few microseconds after plasma initiation. The emission lasts several tens of microseconds with virtually no atomic emission features present beyond about 15 μs. New spectroscopic information as well as peculiar time-evolution patterns of this emission system are obtained.

A. Spectroscopy

After more than one hundred years of nitrogen spectroscopy, the first negative system in N_2^+, i.e., the $B\ ^2\Sigma_u^+\rightarrow X\ ^2\Sigma_g^+$ transition, still attracts experimental and theoretical attention.[18,19] Information on the fine and hyperfine structure of N_2^+ in the (0,1) band of the B-X transition has been obtained in Doppler-tuned laser-induced fluorescence experiments[18] while a long list of spectroscopic constants—including second- and third-order centrifugal distortion constants and off-diagonal matrix elements in the $B\ ^2\Sigma_u^+ - A\ ^2\Pi_u$ Hamiltonian—was generated in a deperturbation study[19(b)] of high-resolution emission data from a specially designed discharge tube.[19(a)]

We report here the observation of line positions in the first negative system of up to $N''=112$ in the R branch—well above the previously obtained lines at $N''=55$.[19(a),19(b)] In mode IIa we have taken many spectra under various excitation conditions and gas pressures. One of the outstanding features in this mode is the excellent reproducibility of the data. Typically, the boxcar integrator delay was set between 10 and 50 μs with a gate width of 1 μs. At these long delay times the overall intensity of the plasma emission has decreased by so much compared to the early times when N^{3+} is observed that further amplification of the photomultiplier output with

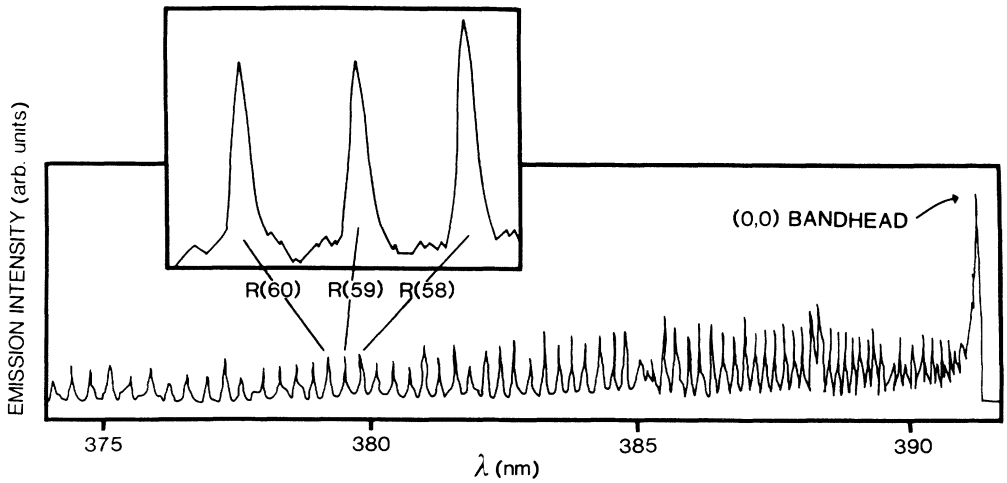

FIG. 3. Wavelength-dispersed emission at 25-μs delay in 550 Torr of N_2 after a 250-mJ laser pulse. Prominent features are the (0,0) bandhead at 391.4 nm and the perturbed region around $N=38$ which also shows up at $N=13$ due to overlap with $P(N+27)$ lines. The spectrum shown was actually continued all the way to the (1,0) bandhead at 358.2 nm with good signal to noise and no detectable emission from the second positive system.

cascaded 100-MHz preamplifiers has to be used. Also, in the spectral region of the $\Delta v=0$ and -1 progressions of the first negative system, no atomic line interference is seen for delay times of more than 15 μs after plasma ignition. In addition, only very weak intensity from the second positive system $C\,^3\Pi_u \rightarrow B\,^3\Pi_g$ of the neutral molecule is present.

Figure 3 is an example of the quality of the data obtainable under typical operation conditions. The pressure in this particular run was 550 Torr of N_2 and the laser-power density was estimated to be about 10^{11} W cm^{-2}. With the laser pulsing at 10 Hz, the monochromator scanning at 1.2 Å/min at a nominal resolution of 0.5 Å, the boxcar was set to average 30 samples. To obtain a scan over the entire $\Delta v=0$ band, the experiment had to accumulate data for about 6 h. After the run was completed, a check for steady-state conditions was performed by remeasuring the bandhead region. Typically, the peak intensity was found to be unchanged to within 10%. Over the entire scan time the laser power and gas pressure were monitored and found to be constant to better than ±2%. Another test for reproducibility consisted in rescanning—under identical experiment parameters—at separate days the same portion of the spectrum. Again, it was found that line position and even line intensities were very well reproduced.

As our wavelength-dispersing instrument is only of low resolution, a complete line-fitting evaluation to obtain improved or additional constants does not seem warranted. However, extra constraints on the third-order distortion constant and perturbation matrix elements for the $v=12$ and 13 of the $A\,^2\Pi_u$ state can be extracted. Rotational perturbation between the $A\,^2\Pi$ and the $B\,^2\Sigma$ states is mediated via spin-orbit and rotation-electronic vibronic interactions which are characterized by the parameters ξ and 2η. Figure 4 demonstrates the quality of the fit between our experimental data and calculated line positions using the spectroscopic values reported in Ref. 19. It is apparent that within the uncertainties of the current experiment there is reasonable agreement for the positions of *all* lines—including the known perturbed lines at around $N=40$ and 65 and the highest, newly observed lines at around $N=110$. An exception are the pronounced deviations localized at $N=82$ and to a lesser extent at $N=95$. These rotational levels are the expected crossing points between the $B\,^2\Sigma(v=0)$ and $A\,^2\Pi(v_A)$ states for $v_A=12$ and 13, respectively, again using the spectroscopic constants in Ref. 19. An attempt was made to vary systematically the corresponding off-diagonal matrix elements in the $^2\Sigma$-$^2\Pi$ Hamiltonian—$\xi+2\eta(1\pm x)$ and $-2\eta(x^2-1)^{1/2}$ with $x=J+\frac{1}{2}$—to obtain the fit between experimental and calculated line positions presented in Fig. 4. The resulting "best-fit" values for $v_A=12$ are $0\le|2\eta|\le 0.1$ and $0\le|\xi|\le 10$ in units of cm^{-1}. A linear correlation between the two perturbation parameters ξ and 2η of the form $\xi\cong 200|\eta|-10$ was evident from our analysis. No such analysis for the weaker $v_A=13$ perturbation was deemed meaningful within the limited resolution of our experiment.

B. Temporal evolution

A typical time dependence of the emission intensity in the first negative system is shown in Fig. 5. This curve is the difference of two runs in mode I (see Sec. II) with the spectrometer tuned to the $N_2^+(B\,^2\Sigma_u^+ \rightarrow X\,^2\Sigma_g^+)$ bandhead at 391.4 nm and a continuous background position nearby. Care was taken that no other emission

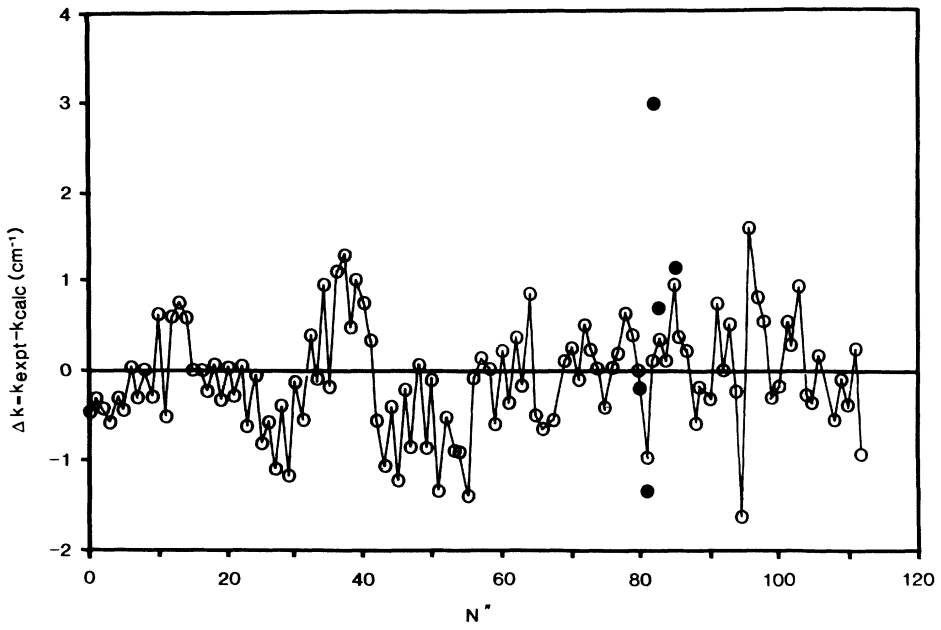

FIG. 4. Difference between observed and calculated line positions in the (0,0) band of the first negative system of N_2^+. Experimental values are from the run shown in Fig. 3; the calculated spectrum is based on spectroscopic constants from Ref. 18(b) including new perturbations due to $A\,^2\Pi_u(v=12)$. Note the large deviation at $N=82$ when no perturbation is assumed (solid circles).

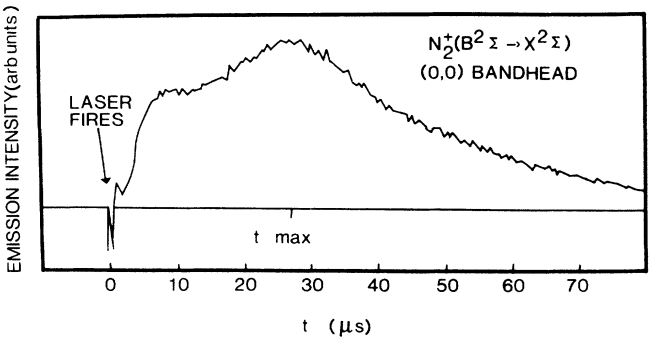

FIG. 5. Time evolution of the $N_2^+(B\text{-}X)$ emission in 550 Torr of N_2 after deposition of 250 mJ at $\lambda=1064$ nm in about 15 ns.

feature—in particular of atomic origin at earlier times—was integrated in these runs. Both of these data sets are the result of averaging 400 laser pulses each. Although insufficient reproducibility leads to spurious peaks at early times, it is obvious—and reliably reproducible—that the first-negative-system emission peaks at around 25 μs. The exact time and intensity of the emission peak depends on nitrogen pressure and laser-power density. Figure 6 summarizes the observed dependence on these parameters. The generic shape of the time evolution as shown in Fig. 5 does not change much with pressure or laser power. One might interpret this shape as the result of two distinct production processes—a fast one within the first few microseconds which levels off at about 10 μs followed by a second, slower "boost phase" which leads to the overall intensity maximum at t_{max}—followed finally by relatively slow decay process at late times.

At 580 Torr—which is the pressure for which many of

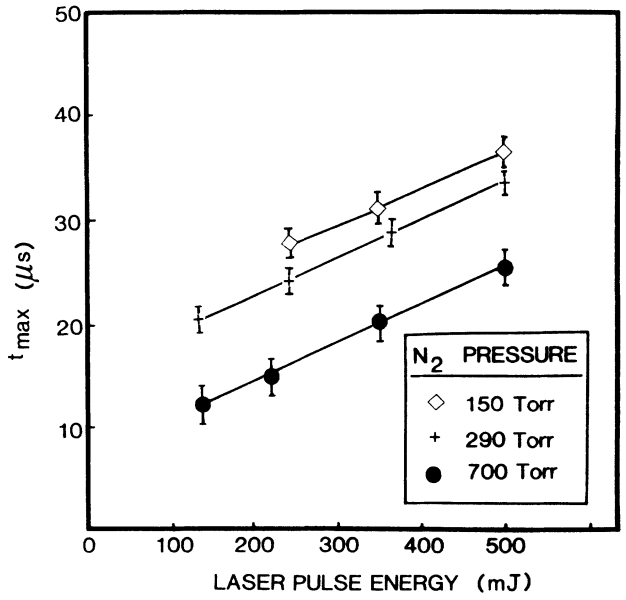

FIG. 6. Influence of laser power and gas pressure on occurrence of intensity peak in $N_2^+(B\text{-}X)$ emission (see Fig. 5).

the data were collected—there are about 50 hard-sphere collisions during the lifetime of the $B\,^2\Sigma_u^+$ state of about 60 ns. It is therefore reasonable to assume that the rovibrational levels of this state are populated according to local thermodynamic equilibrium (LTE). A detailed investigation of emission features in nitrogen plasmas[20] has established relative and absolute intensities observable under LTE conditions. These calculations indicate that the absolute emission intensity (measured, e.g., in number of photons $s^{-1}cm^{-3}$) in the first negative system as a function of temperature has a peak at around 10 000 K. The observed temporal behavior may therefore be just a reflection of the cooling of the laser plasma, and a temperature of about 10 000 K may be expected at delay times of about 20 μs after plasma ignition. Comparing the measured spectra with calculated ones (see Sec. IV A for details on the spectroscopy), it was indeed established that the rotational and vibrational state distribution follows closely a Boltzmann distribution up to the highest detected levels ($N'=112$ and $v'=4$). Figure 7 shows the best-fit calculation to a complete data set taken at a delay of 25 μs and spanning the entire R branch from $N'=1$ to 112. A value of $T_{rot}=9500\pm500$ K is found from such comparisons. At temperatures of 8500 and 10 500 K the calculated spectrum already deviates markedly from the observed data—in particular in the high rotational levels. In the simulation it is assumed that individual lines have triangular line shape with a FWHM determined by the resolution of the monochromator of 0.035 nm. It is well known that in the first negative system of N_2^+, $R(N)$ lines and $P(N+27)$ lines very closely coincide. If the calculated wavelength difference between two such lines (see Sec. IV A for details of the spectroscopy used in determining the line positions) is found to be less than twice the monochromator resolution, i.e., less than 0.07 nm, their corresponding triangular line shapes overlap, and the resulting peak intensity is calculated as the properly weighted sum of the R and P lines. The proper weights are easily computed from the found wavelength difference. The shown calculation reproduces not only the overall shape of the R branch but also many details: for example, the simulation generates the fact that the familiar 2:1 modulation due to the nuclear spin statistic is drastically changed because of the above-mentioned accidential overlap between $R(N)$ and $P(N+27)$ lines and the significant population of high N levels; the fact that this almost perfect (within the instrumental resolution) overlap is lost at various places where perturbations of the $A\,^2\Pi_u$ state shift levels around (lack of overlapping lines shows up as dips in the simulation); and, finally, the fact that below (above) about $N''=30$ odd (even) N'' levels are slightly more intense in both the simulated and the measured spectrum. So, indeed, the observed temperature—which also roughly holds for the vibrational distribution seen in the $\Delta v=-1$ band—at 25-μs delay turns out to be about 10 000 K. However, other experimental runs for delay times ranging from about 15 to 60 μs have shown that the vibration-rotation temperature of the $N_2^+B\,^2\Sigma$ state varies for these delay times only within the current experimental uncertainty. Thus it seems questionable whether the decay at long times can

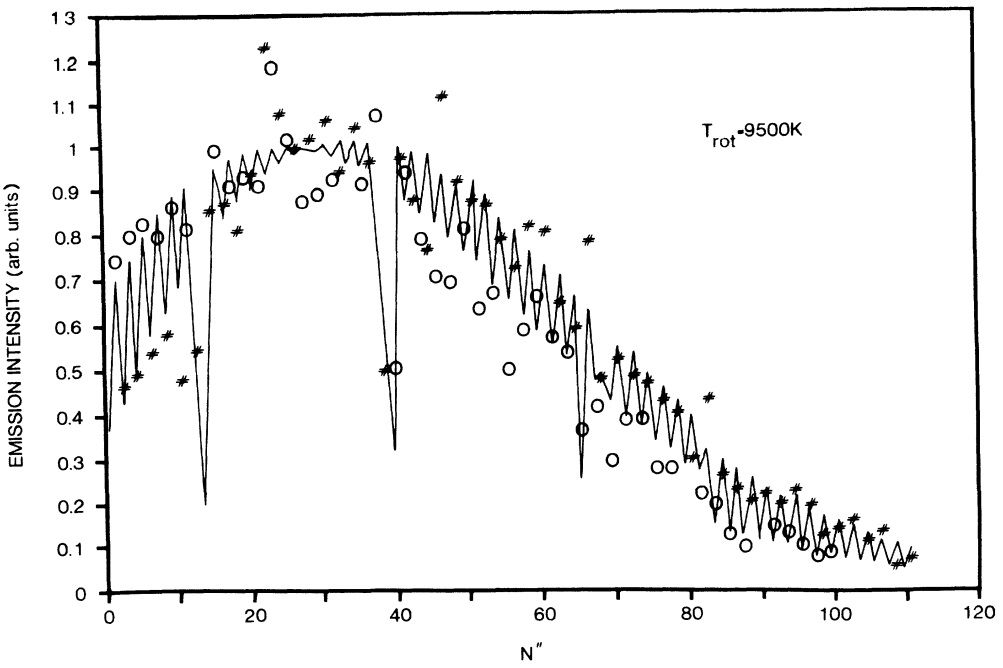

FIG. 7. Experimental (○ represents odd N'', # represents even N'') and calculated emission intensity (solid line) for the data shown in Fig. 3. See text for details.

be explained solely by plasma cooling. More detailed studies—in particular of the high rotational level population—are in progress.

V. SUMMARY

Laser-produced plasmas in pure nitrogen gas at room temperature and pressures ranging from 150 to 700 Torr have been investigated with time-resolved emission spectroscopy. A 10-ns short laser pulse at 1064 nm is focused to a diameter of about 50 μm and delivers up to 500 mJ into the gas. It appears that careful control of the operation parameters allows for very reproducible plasma conditions. Good spatial and temporal resolution result in very clean spectra of unusual spectroscopic features in an otherwise rapidly changing and highly inhomogeneous environment. In particular, the laser-generated plasma is found to contain line emission from N^{3+} atomic ions within the first 100 ns. These lines have been identified at the $3p\ ^3P \rightarrow 3s\ ^3P^\circ$ and the $3p\ ^3P^\circ \rightarrow 3s\ ^3S$ transitions. Their extremely large linewidth is compatible with Stark broadening at electron densities in excess of 10^{18} cm^{-3} which is consistent with full dissociation and ionization of the early plasma. At times later than 20 μs, the plasma emission consists almost entirely of the N_2^+ first negative system, i.e., the $B\ ^2\Sigma_u^+ \rightarrow X\ ^2\Sigma_g^+$ transition. Analysis of the intensity distribution of the rotational lines in the R branch between $N=1$ and 112 indicates a rotational temperature of about 9500 K. The same temperature is consistent with the observed vibrational excitation in the B state. New perturbations in the $B\ ^2\Sigma_u^+$ state at $N=82$ and 95 with, respectively, the $v=12$ and 13 vibrational levels of the $A\ ^2\Pi_u$ state have been observed. The corresponding spin-orbit and rotation-electronic vibronic interaction parameters ξ and 2η were found from best-fit procedures as $0 \leq |\xi| \leq 10$ and $0 \leq |2\eta| \leq 0.1$ for the perturbation with the $v=12$ level.

ACKNOWLEDGMENTS

The authors gratefully acknowledge valuable help from Dr. J. Belliveau in matters of computer interfacing and software support for these experiments.

[1]P. D. Maker, R. W. Terhune, and C. M. Savage, in *Quantum Electronics III*, edited by P. Grivet and N. Bloembergen (Columbia University Press, New York, 1964), p. 1559.

[2]R. W. Minck, J. Appl. Phys. **35**, 252 (1964).

[3]C. DeMichelis, IEEE J. Quantum Electron. **QE-5**, 188 (1969).

[4]H. G. Ahlstrom, J. Phys. (Paris) Colloq. **40**, C7-97 (1979), and also Ref. 6.

[5]*Laser Spectroscopy and Its Applications*, edited by L. J. Radziemski, R. W. Solarz, and J. A. Paisner (Marcel Dekker, New York, 1987).

[6]See, e.g., *Laser Interaction and Related Plasma Phenomena*, edited by H. Hora and G. H. Miley (Plenum, New York, 1988).

[7]R. A. Armstrong, R. A. Lucht, and W. T. Rawlins, Appl. Opt. **22**, 1573 (1983).

[8]D. R. Keefer, B. B. Henriksen, and W. F. Braerman, J. Appl. Phys. **46**, 1080 (1975).

[9]J. Stricker and J. G. Parker, J. Appl. Phys. **53**, 851 (1982).

[10]J. Purić, A. Srećković, S. Djeniže, and M. Platiša, Phys. Rev. A **36**, 3957 (1987).

[11]L. R. Evans and C. G. Morgan, Phys. Rev. Lett. **22**, 1099 (1969).

[12]*MIT Wavelength Tables,* edited by F. M. Phelps (MIT Press, Cambridge, 1982), Vol. 2.

[13]A. l'Huillier, L. A. Lompre, G. Mainfray, and C. Manus, Phys. Rev. A **27**, 2503 (1983).

[14]V. H. S. Kwong, Phys. Rev. A **39**, 4451 (1989), and references therein.

[15]H. R. Griem, *Plasma Spectrocopy* (McGraw-Hill, New York, 1964).

[16]*Plasma Diagnostics,* edited by O. Auciello and D. L. Flamm (Academic, New York, 1989), Vol. 1.

[17]A. W. Ali and E. A. McLean, J. Quant. Spectrosc. Radiat. Transfer **33**, 381 (1985).

[18](a) S. D. Rosner, T. D. Gaily, and R. A. Holt, Phys. Rev. A **26**, 697 (1982); (b) S. D. Rosner, T. D. Gaily, and R. A. Holt, J. Mol. Spectrosc. **109**, 73 (1985).

[19](a) K. A. Dick, W. Benesch, H. M. Crosswhite, S. G. Tilford, R. A. Gottscho, and R. W. Field, J. Mol. Spectrosc. **69**, 95 (1978); (b) R. A. Gottscho, R. W. Field, K. A. Dick, and W. Benesch, *ibid.* **74**, 435 (1979).

[20]W. H. Venable, Jr. and J. B. Shumaker, Jr., J. Quant. Spectrosc. Radiat. Transfer **9**, 1215 (1969).